HHS Public Access

Author manuscript

Glia. Author manuscript; available in PMC 2020 February 10.

Published in final edited form as:

Glia. 2018 July ; 66(7): 1317–1330. doi:10.1002/glia.23313.

Semaphorin4A and H-ferritin utilize Tim-1 on human oligodendrocytes: A novel neuro-immune axis

Brian Chiou[1], **Elisabeth Lucassen**[2], **Michael Sather**[1], **Asha Kallianpur**[3,4], **James Connor**[1]

[1]Department of Neurosurgery, Penn State University College of Medicine, Hershey, Pennsylvania

[2]Department of Neurology, Penn State University College of Medicine, Hershey, Pennsylvania

[3]Department of Genomic Medicine, Cleveland Clinic/Lerner Research Institute, Cleveland, Ohio

[4]Department of Molecular Medicine, Cleveland Clinic Lerner College of Medicine, Case Western Reserve University, Cleveland, Ohio

Abstract

Deficiency of trophic factors relating to the survival of oligodendrocytes, combined with direct interactions with the immune system, are favored paradigms that are increasingly implicated in demyelinating diseases of the central nervous system. We and others have previously shown that Sema4A and H-ferritin interact through the T-cell immunoglobulin and mucin domain (Tim-2) receptor in mice. H-ferritin has been identified as the iron delivery protein for oligodendrocytes, whereas Sema4A causes a direct cytotoxic effect. However, the expression of Tim-2 has not been detected in humans. Here, we demonstrate that, similar to rodents, human oligodendrocytes undergo apoptosis when exposed to Sema4A and take up H-ferritin for meeting iron requirements and that these functions are mediated via the Tim-1 receptor. Moreover, we also demonstrate the ability of H-ferritin to block Sema4A-mediated cytotoxicity. Furthermore, we show in a series of pilot studies that Sema4A is detectable in the CSF of multiple sclerosis patients and HIV-seropositive persons and can induce oligodendrocyte cell death. Together, these results identify a novel iron uptake mechanism for human oligodendrocytes and a connection between oligodendrocytes and the immune system.

Keywords

Apoptosis; demyelination; H-ferritin; multiple sclerosis; oligodendrocyte; semaphorin 4A; Tim-1

1 | INTRODUCTION

Dysregulated myelin production, demyelination, or hypomyelination by oligodendrocytes can lead to a variety of neurological defects, including both motor and cognitive deficits stemming from compromised action potential transmission (Kamm, Uitdehaag, & Polman,

Correspondence: James R. Connor, Department of Neurosurgery, Penn State College of Medicine, 500 University Drive, Hershey, PA, 17033. jrc3@psu.edu.

CONFLICT OF INTEREST STATEMENT

The authors declare no competing financial interests.

2014). One of the primary reasons for irregular myelin deposition may revolve around the death of oligodendrocytes, however the causes for this death have yet to be discovered. Though the brain is normally sequestered from the peripheral immune system, demyelinating disorders may arise as a result of inappropriate interactions between oligodendrocytes and immune cells or trophic factors. In multiple sclerosis, a prototypical demyelinating disorder affecting more than 2.5 million people worldwide (Noseworthy, Lucchinetti, Rodriguez, & Weinshenker, 2000), a number of inflammatory mediators are implicated in demyelination, such as auto-reactive antibodies, infiltrating lymphocytes, and the semaphorin family, suggesting the existence of an oligodendrocyte-immune axis (Leitner, Todorich, Zhang, & Connor, 2015; Okuno, Nakatsuji, & Kumanogoh, 2011; Vadasz & Toubi, 2014).

Human immunodeficiency virus (HIV) infection is another inflammatory condition that has been associated with progressive loss of brain white matter (WM) and neurocognitive impairment (NCI). Although combination antiretroviral therapy (cART) can suppress HIV replication below the quantification limit of commercial assays, comorbidities such as NCI occur more frequently in HIV-seropositive (HIV+) adults than in the general population. NCI is associated with smaller volumes of total WM and larger volumes of abnormal WM in the brain (Fennema-Notestine et al., 2013; Jernigan et al., 2011). These consistently observed WM alterations support the concept that inflammation during immune recovery adversely affects WM integrity. However, the specific molecular mechanisms for these WM changes observed in neuroimaging studies have yet to be defined.

One emerging family of immune-related molecules that have immune-mediated disease properties is the semaphorin family (Vadasz & Toubi, 2014). Implicated in diseases such as rheumatoid arthritis and asthma, the semaphorin family has been shown to be a key component of immune disease progression (Chapoval, Vadasz, Chapoval, & Toubi, 2016; Koda et al., 2014; Mogie et al., 2013; Wang et al., 2015). Importantly, previous studies have shown that Sema4A binds to a member of the T-cell immunoglobulin and mucin domain (Tim) family, Tim-2 (Kumanogoh et al., 2002). Moreover, our laboratory has previously shown that Sema4A causes apoptosis in rodent oligodendrocytes (Leitner et al., 2015). The ability of Sema4A, a significant immune-mediator expressed and secreted by activated T cells, to induce oligodendrocyte cell death is evidence of a key oligodendrocyte-immune axis. Importantly however, the evidence to this point has yet to be translated to humans, representing scientific and clinical gaps in knowledge.

Another binding partner to Tim-2 is the iron storage protein H-ferritin (Hft) (Chen et al., 2005; Han et al., 2011; Todorich, Zhang, Slagle-Webb, Seaman, & Connor, 2008). Historically, transferrin has been thought to be the obligate iron carrier protein throughout the body. However, previous studies by our laboratory have demonstrated the importance of Hft-mediated delivery of iron to oligodendrocytes through Tim-2 (Todorich, Zhang, & Connor, 2011). To oligodendrocytes, iron is a critical micronutrient, as iron is a crucial cofactor in the synthesis and proper deposition of myelin (Connor & Menzies, 1996; Todorich, Pasquini, Garcia, Paez, & Connor, 2009). Indeed, the most consistent observation in the brain in association with iron deficiency is hypomyelination (Franco et al., 2015).

Despite the long-standing interest in establishing an oligodendrocyte-immune system axis, translating the rodent findings for Sema4A and Hft to humans remains challenging primarily because Tim-2 expression has not been detected in humans (Kuchroo, Umetsu, DeKruyff, & Freeman, 2003). The purpose of this study is to demonstrate that Hft is taken up by human oligodendrocytes and Sema4A is toxic to human oligodendrocytes. We hypothesize that Sema4A and Hft both bind to, and are functional at, a shared receptor in humans, likely to be a member of the Tim family. Furthermore, we demonstrate in a series of experiments that Sema4A is found in human CSF and is elevated in human diseases that involve white matter damage, providing an exciting potential clinical link to this pathogenic process. These studies will serve as a crucial impetus for future exploration of Sema4A as a significant clinical factor in demyelinating disorders and H-ferritin as a significant iron delivery protein to human oligodendrocytes.

2 | MATERIALS AND METHODS

2.1 | Cell culture

We used both primary human oligodendrocytes and the human cell line MO3.13, obtained from Cellutions Biosystems Inc. (Ontario, Canada) in the evaluation of Sema4A cytotoxicity and Hft uptake. MO3.13 cells were originally described as a fusion cell line created by fusing human oligodendrocytes obtained from surgical resection of the temporal lobe with human rhabdomyosarcoma cells (Buntinx et al., 2003; McLaurin, Trudel, Shaw, Antel, & Cashman, 1995). These cells were cultured as immature oligodendrocytes in DMEM (Gibco) with 10% FBS and 1× penicillin–streptomycin. Importantly, we differentiated these cells into mature oligodendrocytes by removing serum and culturing cells for 3 days in DMEM containing 100 nM 4-b-phorbol 12-myristate 12-acetate (PMA, Sigma) and 1X penicillin-streptomycin (McLaurin et al., 1995). Mature oligodendrocytes, both primary and MO3.13-derived, express typical differentiated oligodendrocyte markers, such as CC1 and myelin basic protein, while immature cells do not.

Primary human oligodendrocytes were isolated following the protocol outlined by McCarthy and de Vellis (McCarthy & de Vellis, 1980) and Hosokawa (Hosokawa, Klegeris, Maguire, & McGeer, 2003) with minor modifications. Temporal lobe from surgical resection for epilepsy was obtained from two different patients (IRB# 00002914). Briefly, tissues were placed in sterile petri dishes and rinsed with HBSS. Visible blood vessels and meninges were removed and the tissue was chopped into small pieces with a sterile scalpel. Tissue fragments were transferred to a 50 mL tube containing 10 ml 0.25% trypsin (Gibco) and incubated at 37°C for 30 min. 10 ml 10% FBS DMEM-F12 (Sigma) was added to the mixture and the whole suspension was centrifuged at 275g for 10 min. After centrifugation, cells were passed through a 100 μm nylon cell strainer and centrifuged again for 10 min at 275g. Cells were plated on uncoated 10 cm tissue culture plates for 2 hr to allow for microglial adhesion. Following this, non-adherent cells were transferred to a poly-D-lysine coated 10 cm tissue culture plate to adhere astrocytes and incubated for 48 hr. Following this incubation, non-adherent cells were plated onto fresh poly-D-lysine coated plates for mature oligodendrocyte cultures.

2.2 | Cytotoxicity assays

Both MO3.13 and primary human oligodendrocytes were plated at a density of 15,000 cells/well in a 96-well plate format, left to attach overnight. These cells were treated with recombinant Sema4A (Acro-Biosystems) or PBS in increasing doses, added directly to the media for 24 hr. MTT (Roche) and LDH (Roche) assays were performed following the manufacturer's instructions. Absorbance was measured at 575 nm or 490 nm using a Spectramax Gemini plate reader (Molecular Devices). Executioner caspase activity was assayed for using the Caspase-Glo 3/7 Assay (Promega), according to the manufacturer's instructions. The pan-caspase inhibitor Z-VAD-FMK (Selleck Chemicals) was used at 50 μM.

2.3 | Flow cytometry

MO3.13 cells were plated at 1 million cells/well overnight. Sema4A or PBS was added directly to the cells for 4 hr after which cells were harvested. Dual Annexin V/Propidium Iodide (PI) kit (ThermoFisher) was used in conjunction with flow cytometry (FACSCalibur, BD Biosciences) following the manufacturer's instructions to examine for the presence of phosphatidylserine. Ten thousand events were collected and plotted. Only Annexin V positive, PI negative cells were evaluated for statistical significance in the final analysis.

2.4 | H-ferritin purification

Recombinant Hft was isolated as previously described (Fisher et al., 2007; Todorich et al., 2011, 2008). Briefly, wild-type BL21 *Escherichia coli* containing human Hft with a poly-His tag subcloned into pET30a (+) was grown to produce Hft. Isopropyl-β-D-thio-galactoside (IPTG, Sigma) was used to induce expression. Bacteria were then lysed and Hft protein was purified via nickel column using standard techniques (GE Healthcare Bio-Sciences). Total protein was quantified using bicinchoninic acid assay (BCA, Pierce). Hft identity was verified via western blot (*data not shown*).

2.5 | Immunostaining

Human brain tissue (IRB# 40726) was obtained and sectioned in 5-micron slices. Immunohistochemistry and immunofluorescence was performed as previously described (Connor et al., 2011; Nandar et al., 2014). Briefly, slides were deparaffinized and hydrated, performing antigen retrieval with 10mM citrate buffer, pH 6.0. Slides were also blocked in 30% H_2O_2/Methanol for 20 min and 2% non-fat milk made in PBS for 1 hr. Primary antibody was incubated overnight at 4°C, with biotinylated anti-mouse Vectastain ABC kit secondary antibody (Vector Labs) used at 1:200 for IHC. For immunofluorescence, we used fluorescent anti-mouse AlexaFluor 488 antibody in combination with anti-rabbit AlexaFluor 555 antibody at 1:200 to target the anti-CC1 (1:200, Calbiochem), anti-Myelin Basic Protein (MBP, 1:200, Abcam), and anti-Tim-1 (1:200, R&D Systems) antibodies. Immunofluorescence slides were mounted with Prolong Diamond Antifade Mountant with DAPI (ThermoFisher). IHC slides were enhanced using diaminobenzadine (DAB), dehydrated, mounted with Permount, and visualized via light microscope.

Hft protein was conjugated to a red fluorescent quantum dot (Ocean Nanotech) following the manufacturer's protocol. The same protocol was carried out in the absence of Hft,

substituting PBS instead, yielding a negative control (Ctrl-QD). Conjugation was confirmed via gel electrophoresis (*data not shown*). Prior to cell plating, 8-well chamber slides (ThermoFisher) were coated with poly-D-lysine for 2 hr after which the poly-D-lysine was removed and chamber slides dried for 2 hr. 25,000 cells/chamber were then plated overnight. 50 μg Hft-QD or an equivalent volume Ctrl-QD was added to plated cells for 1 hr at 378C. Next, cells were washed three times with 1× DPBS and fixed in 4% paraformaldehyde for 20 min at room temperature. Cells were blocked in 1% milk for 1 hr and stained overnight with an anti-CC1 antibody (Calbiochem) at 1:100. Following this, fluorescent anti-rabbit secondary antibody (Invitrogen) was used at 1:200, counterstaining with DAPI. Cells were visualized on a confocal microscope (Leica). To quantify uptake, differentiated MO3.13 cells were plated at 15,000 cells/well in a 96-well plate. Cells were incubated with Hft-QD or Ctrl-QD for 1 hr at 378C. Subsequently, cells were washed three times with 13 DPBS. Fresh media was added and the signal was counted via fluorometer (Molecular Sciences, Excitation: 420 nm, Emission: 620 nm).

For the Luxol fast blue stain, human tissue slides were deparaffinized, rehydrated to 95% ethanol, and stained in 0.1% Luxol fast blue solution overnight at 56°C. After incubation, slides were rinsed in distilled H_2O and differentiated in 0.05% lithium carbonate solution. Furthermore, slides were counterstained in 0.1% crystal violet solution, dehydrated and mounted. Slides were visualized on a light microscope (Leica).

2.6 | Western blot

Prior to Western blot, total protein was quantified using bicinchoninic assay (BCA, Pierce). A total of 20 mg protein per lane was loaded onto a denaturing SDS-PAGE gel (BioRad) and subsequently transferred to a nitrocellulose membrane. This membrane was blocked in 5% milk made in Tris-buffered saline and Tween-20 (TBS-T). Blots were probed for Tim-1 (10 μg/ml, R&D Systems), Tim-3 (0.1 μg/ml, R&D Systems) or b-actin (1:3000, Sigma) overnight at 4°C. Corresponding secondary antibody conjugated to HRP was used (1:5000, GE Amersham), visualizing bands using ECL reagents (Perkin-Elmer) on an Amersham Imager 600 (GE Amersham) with densitometry analysis using ImageJ.

2.7 | Knockdown studies

To knock down Tim-1 and Tim-3 receptor expression, we used Lipofectamine 3000 (ThermoFisher) to perform the transfections (tfx) per the manufacturer's instructions. To confirm receptor knockdown, 1 million differentiated MO3.13 cells were plated in a 6-well plate overnight. Following this, transfection using either Tim-1, Tim-3, or a scrambled (Scr) pool of siRNA not specific to either Tim proteins (Qiagen) was performed. Cells were lysed in 150 μl RIPA buffer (Sigma), total protein was quantified via BCA, and samples were analyzed via western blot as described above. All other studies were performed in 96-well format, with experiments starting at 24 hr post-transfection. 2,500 ng/well Tim-1 and Tim-3 siRNA (Santa Cruz Biotechnology) were used in the transfections in 6-well, while 100 ng/well siRNA was used in the 96-well transfections.

2.8 | Human CSF samples and immunoprecipitation

Thirteen patients undergoing routine diagnostic lumbar puncture for multiple sclerosis evaluation gave informed consent to Dr. Lucassen (IRB# 00002914). Patient diagnosis was obtained after completion of all studies, thus all laboratory and study personnel were blinded to the status of disease during the experiments. Of the 13 patients evaluated, 5 were diagnosed with multiple sclerosis.

Ten CSF samples were also obtained from HIV+ adults who were previously recruited to multicenter studies of the HIV Neurobehavioral Research Center (HNRC) at the University of California-San Diego (see Acknowledgments). All HIV+ study participants were recruited through community outreach and from health care providers, and they provided written informed consent for lumbar puncture as well as comprehensive neurocognitive and neuropsychiatric testing (HNRC study PI, Robert Heaton, IRB# 081375; Heaton et al., 2011). For the analyses reported here, only samples from HIV+ persons on cART, who did not have AIDS-defining conditions, hepatitis C virus co-infection, or a history of substance abuse or syphilis, were selected for study. In addition, all individuals had a diagnosis of mild or moderately severe NCI, as defined elsewhere (Kallianpur et al., 2016).

CSF Sema4A content was examined using a Sema4A-specific ELISA (Biomatik), following the manufacturer's instructions. Total CSF protein was quantified via BCA. Utilizing Dynabeads Protein A (Invitrogen), 10 μg anti-Sema4A antibody (Abcam) was cross-linked to the magnetic beads using BS3 (Invitrogen). Patient CSF was added to the magnetic bead-antibody solution and incubated at room temperature with gentle agitation for 4 hr. Samples were washed and eluted following the manufacturer's instructions. Identity of the Sema4A product was verified via western blot as described above (*data not shown*).

2.9 | Statistical analysis

All statistical analyses were performed using GraphPad Prism 4 Software (GraphPad Software, Inc.). Data from three independent biological replicates were averaged and are expressed as the mean ± *SD*. Two-way ANOVA with Bonferroni *post-hoc* analysis, unpaired *t* test, Dunnett's or Mann-Whitney tests were used where appropriate to evaluate statistical significance. A p value <.05 was considered significant.

2.10 | Experimental design

Study investigators were blinded to the disease/control status and diagnoses pertaining to CSF samples through a third-party coding mechanism. Patient samples were given a unique coded number while studies were being performed. Only after the studies were finished and the data analyzed were diagnoses revealed to investigators.

3 | RESULTS

The primary cultures were stained with markers for mature oligodendrocytes (CC1 and MBP), astrocytes (GFAP) and microglial cells (Iba1) to identify the cell types present. Only CC1 and MBP immunostained cells were observed. Moreover, these cells also

immunostained for Tim-1 (Figure 1). The positive staining and the morphological appearance of the cells in culture were consistent with oligodendrocytes.

3.1 | Sema4A induces apoptosis in human oligodendrocytes

In order to demonstrate the physiological effects of Sema4A on human oligodendrocytes, we treated the oligodendrocyte cell line MO3.13 as well as primary human oligodendrocytes with increasing doses of Sema4A (Figure 2). In this study, we used primary human oligodendrocytes in addition to the MO3.13 cell line in order to demonstrate similarity in functional response between the two cell types. Similar to our previous studies in rodents (Leitner et al., 2015) and in the mature MO3.13 cell line, Sema4A produced a dose-dependent cytotoxic effect measured by MTT and LDH assay, in both the cell line and primary cells (Figure 2a–c). The cytotoxicity in the MO3.13 cells was only seen in mature cells. We next wanted to study the mechanism of cell death. Given the relatively rapid timeframe of cytotoxicity, we hypothesized that Sema4A induced apoptosis. We found that treatment with Sema4A significantly increases both the amount of Annexin V binding to phosphatidylserine, a marker for early apoptosis, as well as total caspase 3 and 7 activity (Figures 2d,e).

3.2 | H-ferritin is taken up by human oligodendrocytes

Next, we investigated the ability of both the mature MO3.13 cell line and primary human mature oligodendrocytes to take up Hft (Figure 3). For this study, we conjugated red fluorescent quantum dots (QD) to Hft and incubated Hft-QD with the cells. We used a PBS-QD (Ctrl-QD) mixture to control for the random uptake of the QD itself, and did not observe any uptake (Figure 3a). In sharp contrast however, when Hft-QD was incubated with mature MO3.13 and primary oligodendrocytes, a robust uptake was observed (Figure 3b,c). When quantified, Hft-QD uptake (402.95 RFU) was significantly higher than Ctrl-QD uptake (47.40 RFU, p value = .0022, Mann-Whitney test).

3.3 | Human oligodendrocytes express Tim-1

To investigate the role of Tim-1 on the effects by Sema4A and Hft, we first determined the cellular localization of Tim-1 protein expression in the adult human CNS. We stained human brain slices first with Luxol fast blue, a lipid stain used to differentiate between gray matter (GM) and WM (Figure 4a). Staining for Tim-1 in a serial section of the brain tissue demonstrated that Tim-1 was largely located in the WM, with relatively sparse staining in the GM (Figure 4b). Furthermore, upon observation at higher magnification (40×), it is clear that the Tim-1 staining is highly localized to oligodendrocytes, as the cells stained display traditional “tram-track row” arrangement and normal oligodendrocyte morphology (Figure 4c). To verify that the cells immunoreactive for Tim-1 were oligodendrocytes, we performed immunofluorescent staining on human brain slices with anti-CC1 (a mature oligodendrocyte marker) and anti-Tim-1 antibodies (Figure 4d). Colocalization was observed between CC1-positive cells and Tim-1 staining.

3.4 | Tim-1, but not Tim-3, knockdown results in decreased Sema4A cytotoxicity and H-ferritin uptake

Previous studies by our laboratory and others have demonstrated binding of both Sema4A and Hft to Tim-2 (Kumanogoh et al., 2002; Todorich et al., 2008). As previously stated, the gene for Tim-2 has yet to be detected in humans, however candidates for the Hft and Sema4A receptor are likely the other members of the Tim family found in humans, Tim-1 or Tim-3. We chose these receptors based on sequential and structural homology, respectively. Tim-4, the remaining member of the Tim family in humans, was not examined in this study due to a lack of either sequential or structural homology to murine Tim-2 and a lack of expression outside the immune system (Freeman, Casasnovas, Umetsu, & DeKruyff, 2010; Santiago et al., 2007). To assess the possible role of these receptors in Sema4A cytotoxicity, we transfected mature MO3.13 cells with siRNA to knock down the expression of Tim-1 or Tim-3 (Figure 5a,c). As a negative control, we transfected mature MO3.13 cells with a pool of scrambled siRNA. We demonstrate that at 24 hr post-transfection, the protein expression for both Tim-1 and Tim-3 was reduced to roughly 25% (Figure 5b,d). Following this transfection, we treated these cells with Sema4A in increasing doses (Figure 5e). When Tim-3 was knocked down, there was no change in the level of cytotoxicity, compared with the untransfected or scrambled siRNA transfected groups. However, there was a significant rescue of Sema4A cytotoxicity after Tim-1 knockdown.

Given the robust effect of Tim-1 knockdown on Sema4A cytotoxicity, we next examined the role of Tim-1 in Hft uptake by human oligodendrocytes. When Tim-1 expression was knocked down, there was a noticeable decrease in the level of Hft taken up (Figure 6a). However, when the control scrambled siRNA was transfected instead, there was no decline in level of Hft-QD in the cell (Figure 6b). This effect was quantified, demonstrating that after Tim-1 siRNA transfection, uptake of Hft-QD was significantly decreased, whereas Tim-3 siRNA transfection had no noticeable effect compared with the scrambled transfection (Figure 6c).

3.5 | H-ferritin can block Sema4A cytotoxicity

The siRNA studies indicate that Sema4A and Hft share and function through the Tim-1 receptor. To assess the role of Hft in Sema4A cytotoxicity, we treated human oligodendrocytes with both Sema4A and Hft concurrently (Figure 7a). When Sema4A was added alone, there was a similar dose-dependent decrease in cell viability, as seen previously. When Hft was added alone, there was no significant effect on cell viability until the higher concentrations. When we added Hft at a constant dose of 50 μg/ml and Sema4A at increasing doses concurrently (Sema4A + Hft group), there was a rescue effect seen, returning cell viability levels back to control. To corroborate this effect, we used the pan-caspase inhibitor Z-VAD-FMK in order to block the apoptotic effect exerted by Sema4A (Figure 7b). At low doses of Sema4A, this apoptotic effect was completely inhibited. However, at high concentrations, the 50 mM concentration of Z-VAD-FMK was unable to fully reverse this effect.

3.6 | Sema4A from CSF is cytotoxic to oligodendrocytes

Next, we examined the levels and cytotoxic profile of Sema4A in CSF from five patients with multiple sclerosis who underwent routine diagnostic lumbar puncture and from 10 HIV + adults who consented to this procedure as part of previously conducted HIV studies. We first used a Sema4A-specific ELISA on all CSF samples in order to determine levels of Sema4A (Figure 8a). From this experiment, we demonstrated that Sema4A levels are higher in patients diagnosed with multiple sclerosis (86.37 ± 29.99 ng/ml) and in HIV+ individuals (68.50 ± 10.04 ng/ml) compared with HIV-negative, non-multiple sclerosis controls (7.76 ± 2.23 ng/ml; $p < .001$). As mentioned previously, multiple sclerosis patient diagnosis was obtained after all studies were finished, thus all experiments were performed blinded to disease status. We then used a Dynabeads platform coupled to an anti-Sema4A antibody to immunoprecipitate Sema4A from the CSF, resulting in three groups: complete CSF, CSF without Sema4A, and the immunoprecipitated Sema4A. The samples representing these groups were then applied to mature MO3.13 cells and cytotoxicity assessed by LDH assay. Exposing the cells to the immunoprecipitated solution resulted in significant cell death, as compared with the control condition (Figure 8b). Furthermore, the complete CSF mixture was cytotoxic in increasing doses only when Sema4A was present while CSF that had Sema4A levels decreased by immunoprecipitation was less cytotoxic (Figure 8c). These results are also reflected in the larger pool of samples from HIV+ individuals (Figure 8d,e). These data demonstrate that when mature MO3.13 cells are treated with the CSF from HIV1 individuals, there is cell death. When Sema4A was immunoprecipitated from these samples, the cytotoxicity profile was greatly reduced (Figure 8d). Next we examined individual differences in cytotoxicity between CSF with Sema4A and CSF minus Sema4A, finding a decrease in cytotoxicity in 8 out of 10 samples (Figure 8e).

4 | DISCUSSION

The aim of this study was to expand our earlier findings for Sema4A and Hft from animals to humans and find the receptor mediating the interaction of Sema4A and Hft with human oligodendrocytes. Moreover, we demonstrated the presence of Sema4A in human CSF and that the Sema4A in this CSF is cytotoxic to oligodendrocytes. In a cell culture model utilizing both primary human oligodendrocytes and an oligodendrocyte cell line, we have demonstrated a novel role for Sema4A and Hft in humans and evidence for an oligodendrocyte-immune axis that appears informative to demyelinating diseases pathogenesis. Moreover, we provide evidence that Tim-1 is present on human oligodendrocytes in the CNS and is the receptor that mediates these effects.

Building upon our previous studies, we demonstrate that Sema4A is cytotoxic to human oligodendrocytes and is a significant immune factor in CSF that causes apoptosis in oligodendrocytes. That Sema4A induces apoptosis and that this process can be blocked using a pan-caspase inhibitor implies an intracellular signaling cascade leading to executioner caspase activity. Interestingly, immature oligodendrocytes in this study are unaffected by Sema4A treatment; whereas we previously reported the immature MO3.13 cells were less sensitive to Sema4A we did observe cytotoxicity at high doses in that study. This difference in sensitivity to the high doses of Sema4A appear related to cells of higher

passage number being more sensitive. Previous studies of oligodendrocytes have demonstrated that while transferrin receptor is expressed by immature oligodendrocytes, it is absent in mature myelinating oligodendrocytes and adult human brain WM (Bean et al., 2013; Cheng et al., 2015; Hulet, Menzies, & Connor, 2002). This finding corroborates our earlier studies demonstrating ferritin binding in WM tracts in rodents and humans (Hulet, Hess, et al., 1999; Hulet, Heyliger, Powers, & Connor, 2000; Hulet et al., 2002) and other studies demonstrating ferritin binding to oligodendrocytes (Chen et al., 2005; Han et al., 2011; Todorich et al., 2008). The current data, combined with our previous reports, suggest that Tim-1 is expressed on oligodendrocytes during differentiation and by mature oligodendrocytes. This finding is possibly relevant to the presence of transferrin-receptor-positive oligodendrocyte progenitor cells (OPCs), but no ferritin binding, around multiple sclerosis lesions (Connor & Menzies, 1996; Hulet et al., 2000; Wolswijk, 2000) and suggests that as cells in the periplaque region attempt to mature they would become vulnerable to Sema4A..

In addition to Sema4A, we explored the contribution of Hft to oligodendrocyte biology. We have previously demonstrated in rodents that Hft is the preferred source of iron for mature oligodendrocytes, a logical concept given the high iron demands exhibited by myelinating oligodendrocytes and the significantly greater amount of iron that can be delivered via Hft as compared with transferrin-mediated uptake (Todorich et al., 2009, 2011). To date, the human receptor for Hft on oligodendrocytes had not been identified. Torti and colleagues have shown that transferrin receptor 1 (TfR1) can bind to H-ferritin (Li et al., 2010), but the binding was not saturable, unlike the binding of Hft by Tim-2 (Todorich et al., 2008). Moreover, Hft binding to TfR1 inadequately explains iron uptake in oligodendrocytes in adult human WM which lack TfR1 expression (Hulet, Powers, & Connor, 1999). Thus, it is unlikely that TfR1 functions as the receptor for Hft on oligodendrocytes. In this study, we demonstrate using siRNA that human oligodendrocytes take up Hft and that this uptake is mediated through Tim-1. The other candidate in the Tim family that was analyzed was Tim-3 due to the respective sequential and structural homology between Tim-2 and human Tim-1/3 (Kuchroo et al., 2003). Tim-4 was not considered a viable candidate for study because it is exclusively expressed on antigen-presenting cells and thus was not our focus (Freeman et al., 2010).

Though both Sema4A and Hft function through Tim-1, the cellular effects these ligands exert differ greatly. One potential explanation for these differences may be that Sema4A may act as an inhibitor of Hft uptake. As iron is an essential micronutrient to the brain, and oligodendrocytes in particular, the ability of Sema4A to block iron uptake through Hft may contribute to the cell death observed in this study. This may further explain why immature oligodendrocytes are unaffected by Sema4A, as their primary method of iron acquisition is through transferrin, rather than Hft, and thus do not share a receptor with Sema4A. The cytotoxic effect of Hft at higher doses was not unexpected, as it is well-documented that too much iron can also cause cytotoxicity through free radicals and oxidative stress. Though we explored the role of apoptosis in Sema4A mediated cytotoxicity, we fully appreciate that apoptosis and necrosis are not mutually exclusive and that by depriving these cells of iron, both necrosis and apoptosis pathways of cell death may be induced. An alternative explanation for the differing effects of Hft and Sema4A binding may stem from Tim-1 splice

variants, resulting in Tim-1a and Tim-1b (Bailly et al., 2002). Importantly, Tim-1b has the intracellular C-terminal tyrosine phosphorylation motif QAEDNIY while Tim-1a does not, suggesting the ability for Tim-1b to induce intracellular signaling (Bailly et al., 2002). These findings suggest that differential binding of Hft and Sema4A to either Tim-1a or Tim-1b may lead to different downstream effects. Finally, murine Tim-1 and Tim-2 have been shown to form functioning homodimers, suggesting a similar role for human Tim receptors (Santiago et al., 2007). Though the siRNA used in these studies does not discriminate between the Tim-1 splice variants, studies to further explore the mechanism of the different functions of these variants are in progress.

Our study shows significant elevation of Sema4A in the CSF of patients with multiple sclerosis and HIV+ individuals, the first such demonstration and a finding with potentially exciting clinical implications. The Sema4A isolated from this CSF directly causes oligodendrocyte death, providing a potential biomarker of multiple sclerosis disease activity. Although we cannot rule out a contribution from other potentially cytotoxic factors, it is clear from the immunoprecipitation studies that Sema4A is a significant contributor to oligodendrocyte death. Previous studies have linked serum Sema4A levels to multiple sclerosis and therapeutic response (Nakatsuji et al., 2012). For example, interferon-beta treatment is ineffective in relapsing-remitting multiple sclerosis patients, who have both pro-inflammatory T-helper 17 (Th17) cell skewing (Zhou, Chong, & Littman, 2009) and elevated serum Sema4A levels (Koda et al., 2014; Nakatsuji et al., 2012). Moreover, inactivation of Sema4A and Tim-2 signaling decreased the clinical symptoms and histopathological severity of experimental allergic encephalomyelitis (EAE), the mouse model for multiple sclerosis (Kumanogoh et al., 2002). While the source of Sema4A in the CSF examined has yet to be determined, previous findings by our lab have also demonstrated upregulation of Sema4A after microglial activation, providing more evidence for brain immune activation (Leitner et al., 2015). It is also known that Sema4A is present on dendritic cells and CD4+ Th1 cell (Ito & Kumanogoh, 2016). Further studies will examine the exact source of Sema4A found in the brain. The findings from this study require replication using a larger sample size, but it is clear even from the small dataset herein that despite variation in the individual CSF responses, there is a consistent trend that indicates Sema4A is cytotoxic and removal of Sema4A decreases this cytotoxicity. One potential explanation for the individual variability is the Hft to Sema4A ratio present in the CSF. We demonstrated in the cell culture model that Hft can limit Sema4A-mediated cytotoxicity. Hft is not only present in the human CSF (Patton et al., 2017), but in support of the notion that it could impact cytotoxicity has been shown to be protective in HIV persons. Taken together, these findings indicate a role for Sema4A in the pathophysiology of demyelination and a clear relationship between Tim-1, iron uptake in oligodendrocytes, and the immune system.

In addition, this study is the first to suggest a role for Sema4A in demyelinating neurological diseases other than multiple sclerosis, in particular, HIV-associated NCI (Liu, Xu, Liu, & Xiong, 2016). Damage to WM is detected early in the course of HIV infection (Ragin et al., 2015) and is clearly related to the duration and severity of immunosuppression, as reflected by a lower CD4+ T-cell nadir, but several studies suggest that immune recovery may also play an independent role in the evolution of brain abnormalities and NCI (Fennema-Notestine et al., 2013). Specifically, reduced WM integrity on neuroimaging is associated

with higher current and lower nadir $CD4^+$ T-cell counts (Fennema-Notestine et al., 2013; Gongvatana et al., 2013; Jernigan et al., 2011; Seider et al., 2016; Zhu et al., 2013). Fennema-Notestine et al. showed that HIV+ adults experienced significant loss of total cerebral WM volume, alongside increases in abnormal WM volume. These consistently observed WM alterations, which may progress as the CD4+ T-cell count recovers during cART, could potentially contribute to NCI. These studies suggest that inflammation during immune recovery on cART adversely affects cerebral WM integrity, but other mechanisms of WM damage have not been sufficiently investigated; our findings implicate increased levels of Sema4A as another possible mechanism, requiring further study. Additional studies further investigating a role for Sema4A in HIV neuropathogenesis are currently underway.

Overall, the data presented in this study provide evidence for a novel neuro-immune axis between oligodendrocytes in the brain and the immune trophic factor Sema4A. Importantly, these studies have elucidated a novel and significant receptor for Sema4A and Hft on oligodendrocytes. In preliminary studies, we also provide exciting evidence for a clinical link between demyelinating disorders and Sema4A levels.

ACKNOWLEDGMENT

This work was supported by the Department of Neurosurgery at Penn State College of Medicine and the G. M. Leader Family Research Fund. The San Diego HIV Neurobehavioral Research Center [HNRC] is supported by Center award P30MH062512 from NIMH. We also thank Drs. A. B. Madhankumar, Amanda Snyder, and David Degraff for their role in providing technical expertise and guidance. We are also grateful to the study participants who provided HIV1 CSF for these studies. The HNRC is affiliated with the University of California, San Diego, the Naval Hospital, San Diego, and the Veterans Affairs San Diego Healthcare System, and includes: Director: Robert K. Heaton, PhD, Co-Director: Igor Grant, MD; Associate Directors: J. Hampton Atkinson, MD, Ronald J. Ellis, MD, PhD, and Scott Letendre, MD; Center Manager: Thomas D. Marcotte, PhD; Jennifer Marquie-Beck, MPH; Melanie Sherman; *Neuromedical Component*: Ronald J. Ellis, MD, PhD (P. I.), Scott Letendre, MD, J. Allen McCutchan, MD, Brookie Best, PharmD, Rachel Schrier, PhD, Debra Rosario, MPH; *Neurobehavioral Component*: Robert K. Heaton, PhD (P. I.), J. Hampton Atkinson, MD, Thomas D. Marcotte, PhD, Mariana Cherner, PhD, David J. Moore, PhD, Erin Morgan, PhD, Matthew Dawson; *Neuroimaging Component*: Christine Fennema-Notestine, PhD (P. I.), Monte S. Buchsbaum, MD, John Hesselink, MD, Sarah L. Archibald, MA, Gregory Brown, PhD, Richard Buxton, PhD, Anders Dale, PhD, Thomas Liu, PhD; *Neurobiology Component*: Eliezer Masliah, MD (P. I.), Cristian Achim, MD, PhD; *Neurovirology Component*: David M. Smith, MD (P. I.), Douglas Richman, MD; International Component: J. Allen McCutchan, MD, (P. I.), Mariana Cherner, PhD; *Developmental Component*: Cristian Achim, MD, PhD; (P. I.), Scott Letendre, MD; *Participant Accrual and Retention Unit*: J. Hampton Atkinson, MD (P. I.), Jennifer Marquie-Beck, MPH; Data *Management and Information Systems Unit*: Anthony C. Gamst, PhD (P. I.), Clint Cushman; *Statistics Unit*: Ian Abramson, PhD (P. I.), Florin Vaida, PhD (Co-PI), Anya Umlauf, MS, Bin Tang, MS. The views expressed in this article are those of the authors and do not reflect the official policy or position of the Department of the Navy, Department of Defense, nor the United States Government.

REFERENCES

Bailly V, Zhang Z, Meier W, Cate R, Sanicola M, & Bonventre JV (2002). Shedding of kidney injury molecule-1, a putative adhesion protein involved in renal regeneration. Journal of Biological Chemistry, 277(42), 39739–39748. 10.1074/jbc.M200562200 [PubMed: 12138159]

Bean GR, Ganesan YT, Dong Y, Takeda S, Liu H, Chan PM, … Cheng EH-Y (2013). PUMA and BIM are required for oncogene inactivation-induced apoptosis. Science Signaling, 6(268), ra20–ra23. 10.1126/scisignal.2003483 [PubMed: 23532334]

Buntinx M, Vanderlocht J, Hellings N, Vandenabeele F, Lambrichts I, Raus J, … Steels P (2003). Characterization of three human oligodendroglial cell lines. Journal of Neurocytology, 32(1), 25–38. [PubMed: 14618099]

Chapoval SP, Vadasz Z, Chapoval AI, & Toubi E (2016). Semaphorins 4A and 4D in chronic inflammatory diseases. Inflammation Research, 1–7. 10.1007/s00011-016-0983-5

Chen TT, Li L, Chung D-H, Allen CDC, Torti SV, Torti FM, … Daws MR (2005). TIM-2 is expressed on B cells and in liver and kidney and is a receptor for H-ferritin endocytosis. The Journal of Experimental Medicine, 202(7), 955–965. 10.1084/jem.20042433 [PubMed: 16203866]

Cheng H-T, Yen C-J, Chang C-C, Huang K-T, Chen K-H, Zhang R-Y, … Hung K-Y (2015). Ferritin heavy chain mediates the protective effect of heme oxygenase-1 against oxidative stress. Biochimica Et Biophysica Acta, 1850(12), 2506–2517. 10.1016/j.bbagen.2015.09.018 [PubMed: 26423448]

Connor JR, & Menzies SL (1996). Relationship of iron to oligodendrocytes and myelination. Glia, 17(2), 83–93. 10.1002/(SICI)1098-1136(199606)17:2<83::AID-GLIA1>3.0.CO;2-7 [PubMed: 8776576]

Connor JR, Ponnuru P, Wang X-S, Patton SM, Allen RP, Earley CJ, & Leader GM (2011). Profile of altered brain iron acquisition in restless legs syndrome. Brain, 134(4), 959–968. 10.1093/brain/awr012 [PubMed: 21398376]

Fennema-Notestine C, Ellis RJ, Archibald SL, Jernigan TL, Letendre SL, Notestine RJ, … Grant I (2013). Increases in brain white matter abnormalities and subcortical gray matter are linked to CD4 recovery in HIV infection. Journal of Neurovirology, 19(4), 393–401. 10.1007/s13365-013-0185-7 [PubMed: 23838849]

Fisher J, Devraj K, Ingram J, Slagle-Webb B, Madhankumar AB, Liu X, … Connor JR (2007). Ferritin: A novel mechanism for delivery of iron to the brain and other organs. American Journal of Physiology. Cell Physiology, 293(2), C641–C649. 10.1152/ajpcell.00599.2006 [PubMed: 17459943]

Franco PG, Pasquini LA, Perez MJ, Rosato-Siri MV, Silvestroff L, & Pasquini JM (2015). Paving the way for adequate myelination: The contribution of galectin-3, transferrin and iron. FEBS Letters, 589 (22), 3388–3395. 10.1016/j.febslet.2015.08.001 [PubMed: 26296311]

Freeman GJ, Casasnovas JM, Umetsu DT, & DeKruyff RH (2010). TIM genes: A family of cell surface phosphatidylserine receptors that regulate innate and adaptive immunity. Immunological Reviews, 235(1), 172–189. 10.1111/j.0105-2896.2010.00903.x [PubMed: 20536563]

Gongvatana A, Harezlak J, Buchthal S, Daar E, Schifitto G, Campbell T, … Navia B (2013). Progressive cerebral injury in the setting of chronic HIV infection and antiretroviral therapy. Journal of Neurovirology, 19(3), 209–218. 10.1007/s13365-013-0162-1 [PubMed: 23613008]

Han J, Seaman WE, Di X, Wang W, Willingham M, Torti FM, & Torti SV (2011). Iron uptake mediated by binding of H-ferritin to the TIM-2 receptor in mouse cells. PLoS ONE, 6(8), e23800–e23809. 10.1371/journal.pone.0023800 [PubMed: 21886823]

Heaton RK, Franklin DR, Ellis RJ, McCutchan JA, Letendre SL, LeBlanc S, … Grant I (2011). HIV-associated neurocognitive disorders before and during the era of combination antiretroviral therapy: Differences in rates, nature, and predictors. Journal of Neurovirology, 17(1), 3–16. 10.1007/s13365-010-0006-1 [PubMed: 21174240]

Hosokawa M, Klegeris A, Maguire J, & McGeer PL (2003). Expression of complement messenger RNAs and proteins by human oligodendroglial cells. Glia, 42(4), 417–423. 10.1002/glia.10234 [PubMed: 12730962]

Hulet S, Hess E, Debinski W, Arosio P, Bruce K, Powers S, & Connor JR (1999). Characterization and distribution of ferritin binding sites in the adult mouse brain. Journal of Neurochemistry, 72(2), 868–874. 10.1046/j.1471-4159.1999.720868.x [PubMed: 9930764]

Hulet S, Heyliger S, Powers S, & Connor J (2000). Oligodendrocyte progenitor cells internalize ferritin via clathrin-dependent receptor mediated endocytosis. Journal of Neuroscience Research, 61(1), 52–60. 10.1002/1097-4547(20000701)61:1<52::AIDJNR6>3.0.CO;2-T [pii] [PubMed: 10861799]

Hulet S, Powers S, & Connor J (1999). Distribution of transferrin and ferritin binding in normal and multiple sclerotic human brains. Journal of the Neurological Sciences, 165(1), 48–55. 10.1016/S0022-510X(99)00077-5 [PubMed: 10426147]

Hulet SW, Menzies S, & Connor JR (2002). Ferritin binding in the developing mouse brain follows a pattern similar to myelination and is unaffected by the jimpy mutation. Developmental Neuroscience, 24 (2–3), 208–213. http://doi.org/65704 [PubMed: 12401960]

Ito D, & Kumanogoh A (2016). The role of Sema4A in angiogenesis, immune responses, carcinogenesis, and retinal systems. Cell Adhesion & Migration, 10(6), 692–699. 10.1080/19336918.2016.1215785 [PubMed: 27736304]

Jernigan TL, Archibald SL, Fennema-Notestine C, Taylor MJ, Theilmann RJ, Julaton MD, … Grant I (2011). Clinical factors related to brain structure in HIV: The CHARTER study. Journal of Neurovirology, 17(3), 248–257. 10.1007/s13365-011-0032-7 [PubMed: 21544705]

Kallianpur AR, Wang Q, Jia P, Hulgan T, Zhao Z, Letendre SL, … Grant I (2016). Anemia and red blood cell indices predict HIV-associated neurocognitive impairment in the highly active antiretroviral therapy era. Journal of Infectious Diseases, 213(7), 1065–1073. 10.1093/infdis/jiv754 [PubMed: 26690344]

Kamm CP, Uitdehaag BM, & Polman CH (2014). Multiple sclerosis: Current knowledge and future outlook. European Neurology, 72(3–4), 132–141. 10.1159/000360528 [PubMed: 25095894]

Koda T, Okuno T, Takata K, Honorat JA, Kinoshita M, Tada S, … Nakatsuji Y (2014). Sema4A inhibits the therapeutic effect of IFN-b in EAE. Journal of Neuroimmunology, 268(1–2), 43–49. 10.1016/j.jneuroim.2013.12.014 [PubMed: 24439904]

Kuchroo VK, Umetsu DT, DeKruyff RH, & Freeman GJ (2003). The TIM gene family: Emerging roles in immunity and disease. Nature Reviews Immunology, 3(6), 454–462. 10.1038/nri1111

Kumanogoh A, Marukawa S, Suzuki K, Takegahara N, Watanabe C, Ch'ng ESeng, … Kikutani H (2002). Class IV semaphorin Sema4A enhances T-cell activation and interacts with Tim-2. Nature, 419 (6907), 629–633. 10.1038/nature01037 [PubMed: 12374982]

Leitner DF, Todorich B, Zhang X, & Connor JR (2015). Semaphorin4A is cytotoxic to oligodendrocytes and is elevated in microglia and multiple sclerosis. ASN Neuro, 7(3), 1–13. 10.1177/1759091415587502

Li L, Fang CJ, Ryan JC, Niemi EC, Lebron JA, Bjorkman PJ, … Seaman WE (2010). Binding and uptake of H-ferritin are mediated by human transferrin receptor-1. Proceedings of the National Academy of Sciences of the United States of America, 107(8), 3505–3510. 10.1073/pnas.0913192107 [PubMed: 20133674]

Liu H, Xu E, Liu J, & Xiong H (2016). Oligodendrocyte injury and pathogenesis of HIV-1-associated neurocognitive disorders. Brain Sciences, 6(4), 23 (10.3390/brainsci6030023

McCarthy KD, & de Vellis J (1980). Preparation of separate astroglial and oligodendroglial cell cultures from rat cerebral tissue. The Journal of Cell Biology, 85(3), 890–902. http://doi.org/0021-9525/80 [PubMed: 6248568]

McLaurin J, Trudel GC, Shaw IT, Antel JP, & Cashman NR (1995). A human glial hybrid cell line differentially expressing genes subserving oligodendrocyte and astrocyte phenotype. Journal of Neurobiology, 26(2), 283–293. 10.1002/neu.480260212 [PubMed: 7707048]

Mogie G, Shanks K, Nkyimbeng-Takwi EH, Smith E, Davila E, Lipsky MM, … Chapoval SP (2013). Neuroimmune semaphorin 4A as a drug and drug target for asthma. International Immunopharmacology, 17(3), 568–575. 10.1016/j.intimp.2013.08.005 [PubMed: 23994348]

Nakatsuji Y, Okuno T, Moriya M, Sugimoto T, Kinoshita M, Takamatsu H, … Kumanogoh A (2012). Elevation of Sema4A implicates Th cell skewing and the efficacy of IFN-b therapy in multiple sclerosis. Journal of Immunology, 188(10), 4858–4865. 10.4049/jimmunol.1102023

Nandar W, Neely EB, Simmons Z, & Connor JR (2014). H63D HFE genotype accelerates disease progression in animal models of amyotrophic lateral sclerosis. Biochimica Et Biophysica Acta – Molecular Basis of Disease, 1842(12), 2413–2426. 10.1016/j.bbadis.2014.09.016

Noseworthy JH, Lucchinetti C, Rodriguez M, & Weinshenker BG (2000). Multiple sclerosis. The New England Journal of Medicine, 343 (13), 938–952. 10.1056/NEJM200009283431307 [PubMed: 11006371]

Okuno T, Nakatsuji Y, & Kumanogoh A (2011). The role of immune semaphorins in multiple sclerosis. FEBS Letters, 585(23), 3829–3835. 10.1016/j.febslet.2011.03.033 [PubMed: 21420960]

Patton SM, Wang Q, Hulgan T, Connor JR, Jia P, Zhao Z, … Kallianpur AR (2017). Cerebrospinal fluid (CSF) biomarkers of iron status are associated with CSF viral load, antiretroviral therapy, and demographic factors in HIV-infected adults. Fluids and Barriers of the CNS, 14(1), 11 10.1186/s12987-017-0058-1 [PubMed: 28427421]

Ragin AB, Wu Y, Gao Y, Keating S, Du H, Sammet C, … Epstein LG (2015). Brain alterations within the first 100 days of HIV infection. Annals of Clinical and Translational Neurology, 2(1), 12–21. 10.1002/acn3.136 [PubMed: 25642430]

Santiago C, Ballesteros A, Tami C, Martínez-Muñoz L, Kaplan GG, & Casasnovas JM (2007). Structures of T cell immunoglobulin mucin receptors 1 and 2 reveal mechanisms for regulation of immune responses by the Tim receptor family. Immunity, 26(3), 299–310. 10.1016/j.immuni.2007.01.014 [PubMed: 17363299]

Seider TR, Gongvatana A, Woods AJ, Chen H, Porges EC, Cummings T, … Cohen RA (2016). Age exacerbates HIV-associated white matter abnormalities. Journal of Neurovirology, 22(2), 201–212. 10.1007/s13365-015-0386-3 [PubMed: 26446690]

Todorich B, Pasquini JM, Garcia CI, Paez PM, & Connor JR (2009). Oligodendrocytes and myelination: The role of iron. GLIA, 57 (5), 467–478. 10.1002/glia.20784 [PubMed: 18837051]

Todorich B, Zhang X, & Connor JR (2011). H-ferritin is the major source of iron for oligodendrocytes. Glia, 59(6), 927–935. 10.1002/glia.21164 [PubMed: 21446040]

Todorich B, Zhang X, Slagle-Webb B, Seaman WE, & Connor JR (2008). Tim-2 is the receptor for H-ferritin on oligodendrocytes. Journal of Neurochemistry, 107(6), 1495–1505. 10.1111/j.1471-4159.2008.05678.x [PubMed: 19014383]

Vadasz Z, & Toubi E (2014). Semaphorins: Their dual role in regulating immune-mediated diseases. Clinical Reviews in Allergy & Immunology, 47(1), 17–25. 10.1007/s12016-013-8360-4 [PubMed: 23397481]

Wang L, Song G, Zheng Y, Tan W, Pan J, Zhao Y, & Chang X (2015). Expression of Semaphorin 4A and its potential role in rheumatoid arthritis. Arthritis Research & Therapy, 17(1), 227 10.1186/s13075-015-0734-y [PubMed: 26303122]

Wolswijk G (2000). Oligodendrocyte survival, loss and birth in lesions of chronic-stage multiple sclerosis. Brain, 123(1), 105–115. 10.1093/brain/123.1.105 [PubMed: 10611125]

Zhou L, Chong MMW, & Littman DR (2009). Plasticity of CD4+ T cell lineage differentiation. Immunity, 30(5), 646–655. 10.1016/j.immuni.2009.05.001 [PubMed: 19464987]

Zhu T, Zhong J, Hu R, Tivarus M, Ekholm S, Harezlak J, … Schifitto G (2013). Patterns of white matter injury in HIV infection after partial immune reconstitution: A DTI tract-based spatial statistics study. Journal of Neurovirology, 19(1), 10–23. 10.1007/s13365-012-0135-9. [PubMed: 23179680]

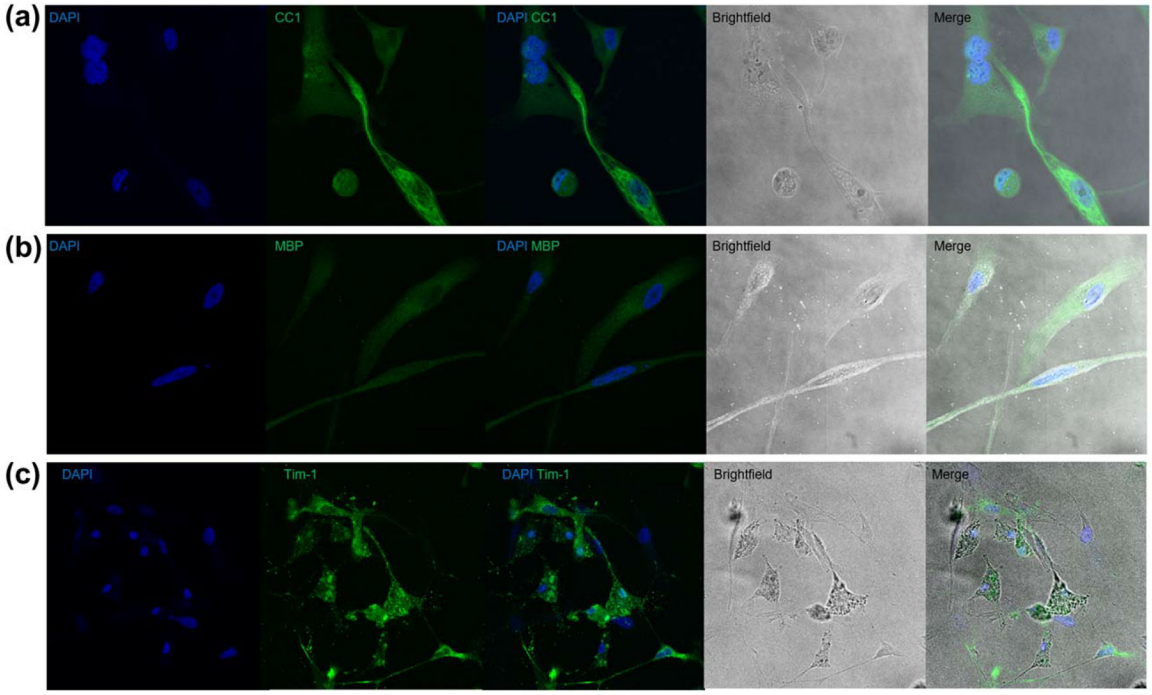

FIGURE 1.

Characterization of isolated primary human oligodendrocytes. Isolated oligodendrocytes express CC1 (a) and MBP (b), both markers of mature myelinating oligodendrocytes. Furthermore, these cells also express Tim-1 (c). All images were taken at 63X magnification

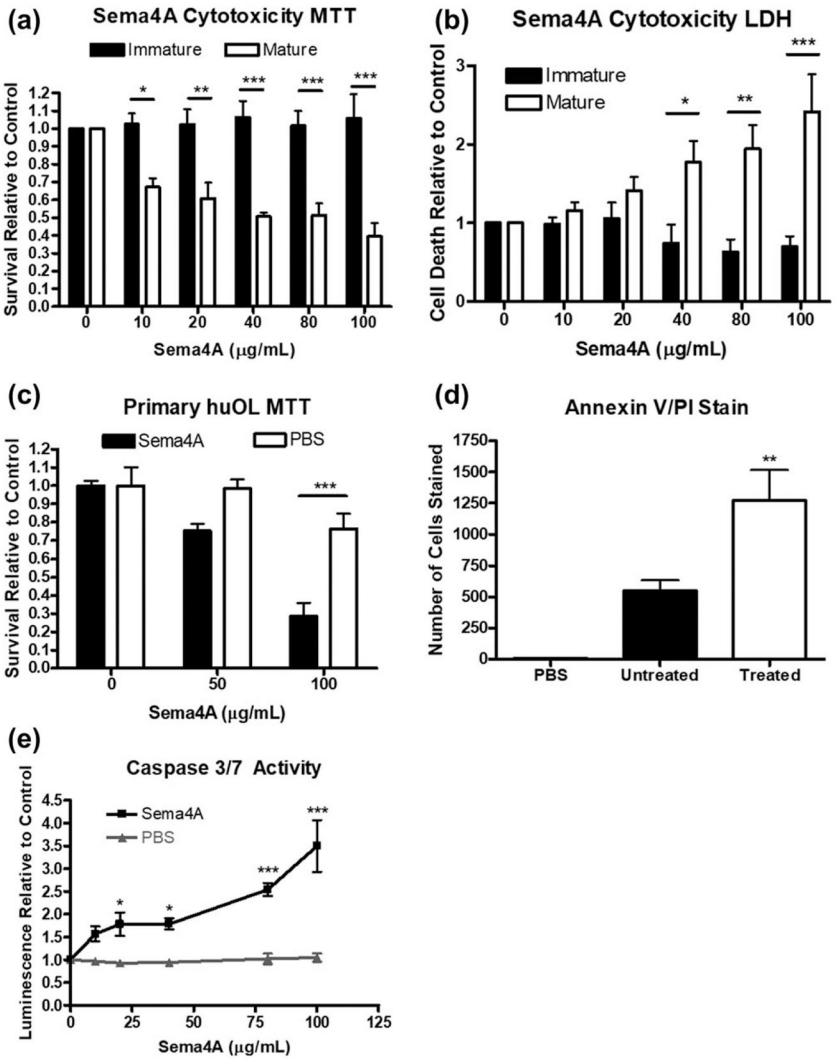

FIGURE 2.

Sema4A causes a dose dependent increase in apoptosis. (a and b) Sema4A causes cell death in mature, but not immature, human oligodendrocyte cell line MO3.13. (c) Sema4A causes cell death in primary human oligodendrocytes. (d) Annexin V positive, Propidium Iodide (PI) negative binding is increased in the presence of 40 μg/ml Sema4A ($p = .0028$, one-way ANOVA). (e) Caspases 3 and 7 are activated after Sema4A incubation in increasing doses. In all experiments, absorbance is quantified against the untreated or PBS controls. Means were evaluated for statistical significance using two-way ANOVA with Bonferroni's post hoc comparisons. Values represent means of three biological replicates ± *SD*. *$p < .05$, **$p < .01$, ***$p < .001$

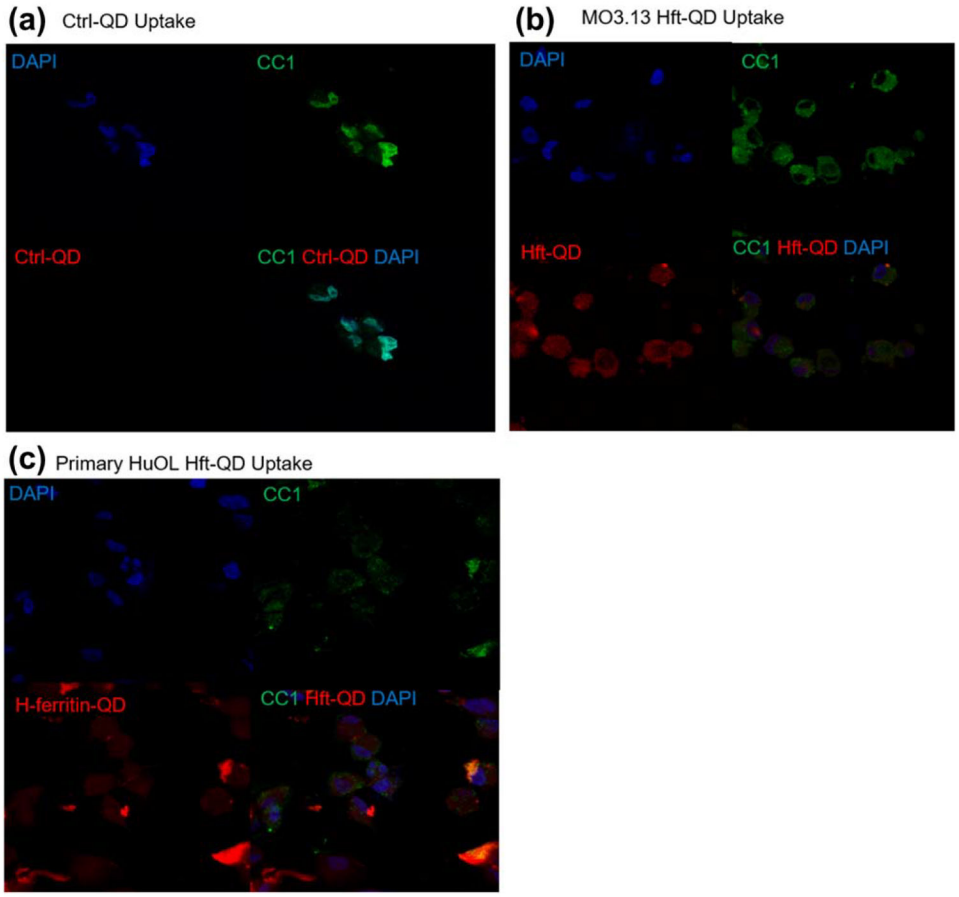

FIGURE 3.

Human oligodendrocytes take up H-ferritin. (a) A negative control quantum dot (QD) is not taken up by mature MO3.13 cells. (b) Mature MO3.13 cells take up H-ferritin labeled with a red fluorescent QD. (c) Primary human oligodendrocytes take up Hft-QD. CC1 staining represents mature oligodendrocytes while DAPI staining was used as a nuclear stain. All images were taken at 63X magnification

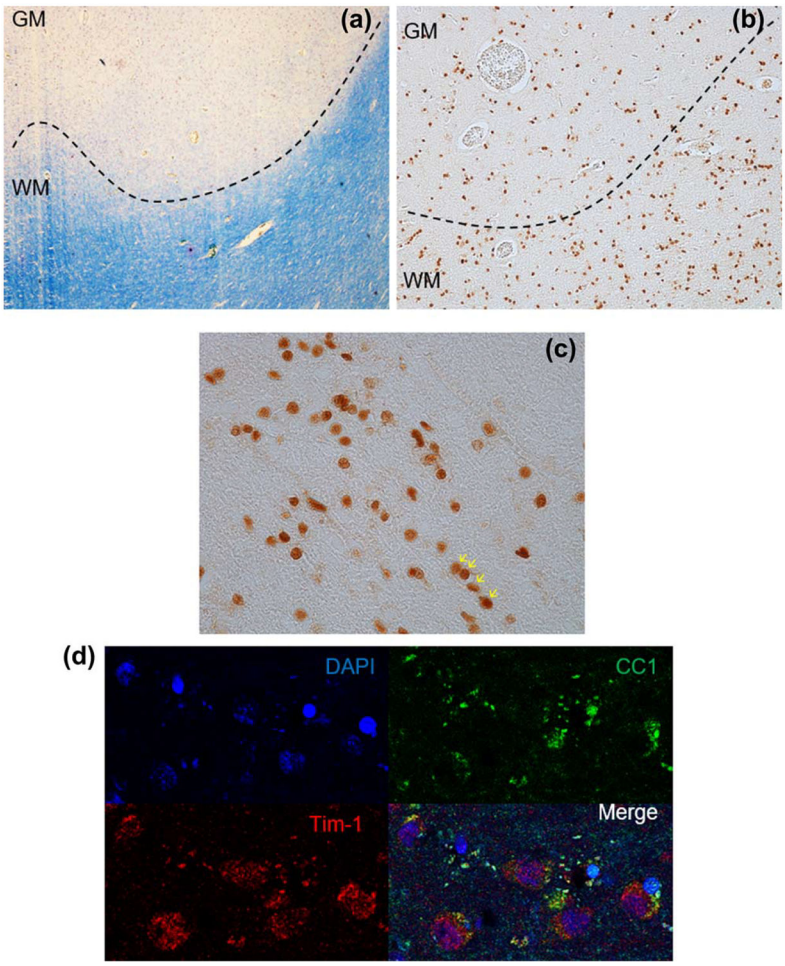

FIGURE 4.

Human oligodendrocytes express Tim-1. (a) Luxol fast blue staining on human brain tissue demonstrating gray matter (GM) and white matter (WM) border, 2× magnification. (b) DAB-enhanced stain of Tim-1 in the same region, 10× magnification. (c) 40× magnification of Tim-1 stain, yellow arrows demonstrating classic “tram-track” oligodendrocyte morphology and arrangement. (d) Immunofluorescence colocalization between Tim-1 and CC1 demonstrating oligodendrocyte expression of Tim-1

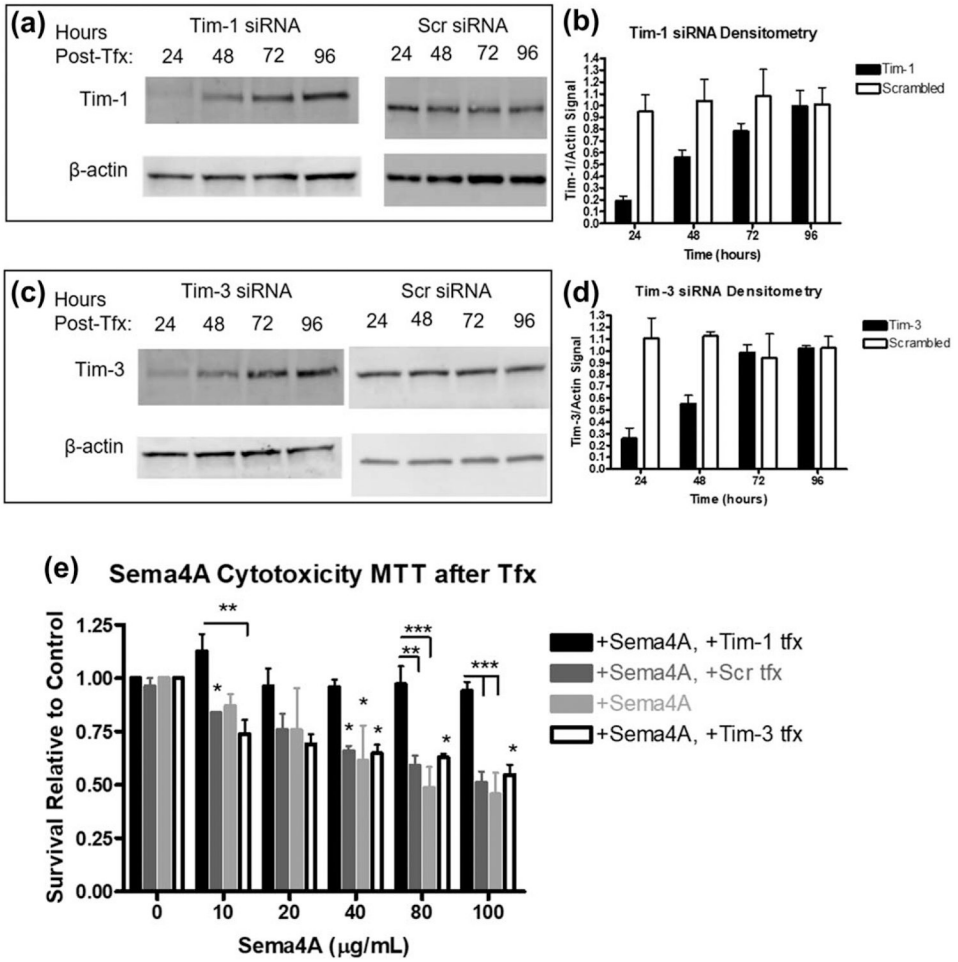

FIGURE 5.

Tim-1 knockdown results in decreased Sema4A cytotoxicity. (a) Western blot results of Tim-1 knockdown. (b) Tim-1 is most effectively knocked down after 24 hr. (c) Western blot results of Tim-3 knockdown. (d) Tim-3 is most effectively knocked down after 24 hr. (e) Tim-1, but not Tim-3, knockdown results in a protection from Sema4A-mediated cytotoxicity. Means were evaluated for statistical significance using two-way ANOVA with Bonferroni's post hoc comparisons. Graphs represent means of three biological replicates ± *SD*. *$p < .05$, **$p < .01$, ***$p < .001$ where * refers to comparisons between the experimental group and the +Sema4A and +Tim-1 tfx condition

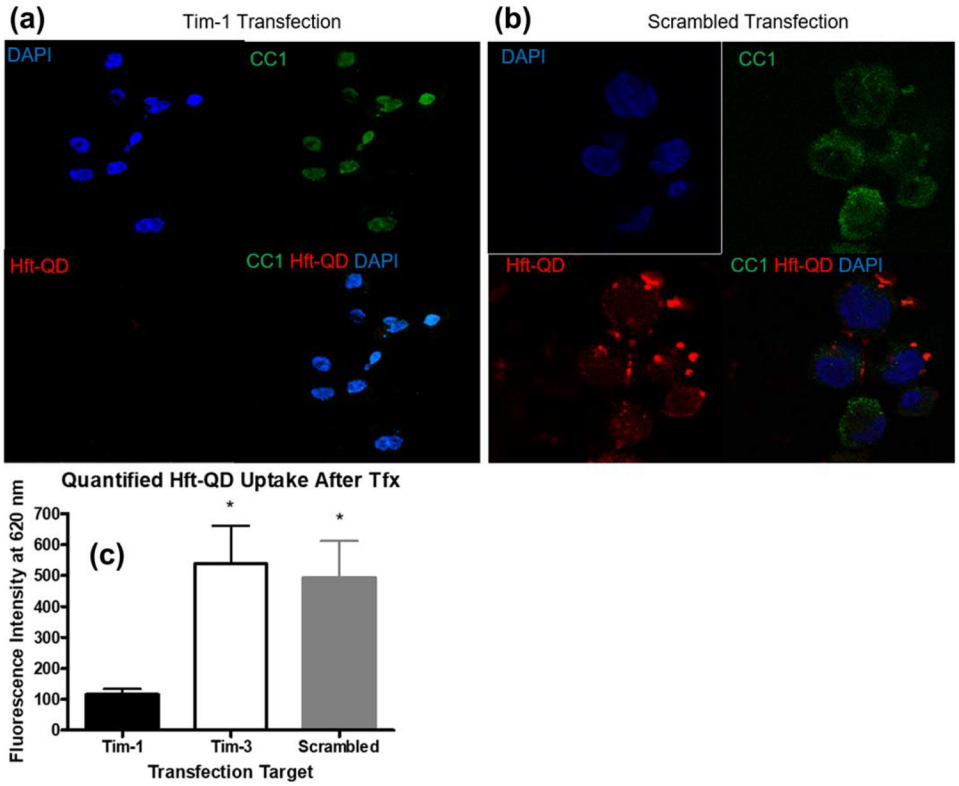

FIGURE 6.

Tim-1 knockdown results in decreased H-ferritin uptake. (a) Tim-1 knockdown decreases the amount of Hft-QD taken up by mature MO3.13 cells. (b) Scrambled siRNA knockdown does not affect Hft-QD uptake. (c) Tim-1, but not Tim-3 or scrambled, knockdown decreases Hft-QD uptake. All images were taken at 63X magnification. Means were evaluated for statistical significance using one-way ANOVA with Dunnett's Multiple Comparison Test. Values represent means of three biological replicates ± *SD*. *$p < .05$

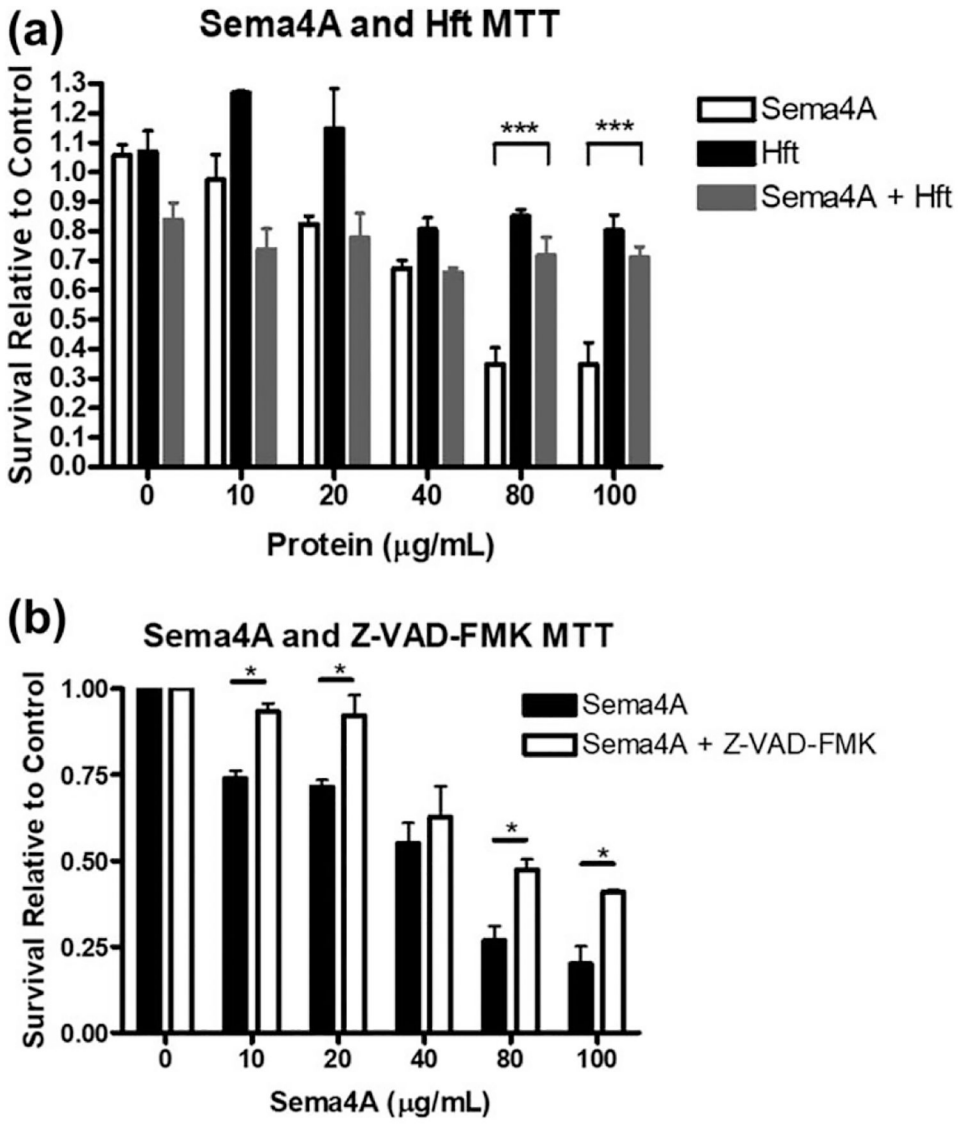

FIGURE 7.

Sema4A cytotoxicity is blocked by H-ferritin or caspase inhibition. (a) H-ferritin can block Sema4A cytotoxicity, when compared with Sema4A alone or Hft alone conditions. Absorbance is quantified relative to a PBS control condition (*not shown*). In the Sema4A + Hft condition, Hft concentration was added at a constant 50 μg/ml while Sema4A was added in increasing doses as labeled. (b) Z-VAD-FMK, a pan-caspase inhibitor, can block Sema4A cytotoxicity. This rescue effect is diminished at high concentrations of Sema4A. Absorbance is quantified relative to the untreated control. Means were evaluated for statistical significance using two-way ANOVA with Bonferroni's post hoc comparisons. Values represent means of three biological replicates ± *SD*. *$p < .05$, ***$p < .001$

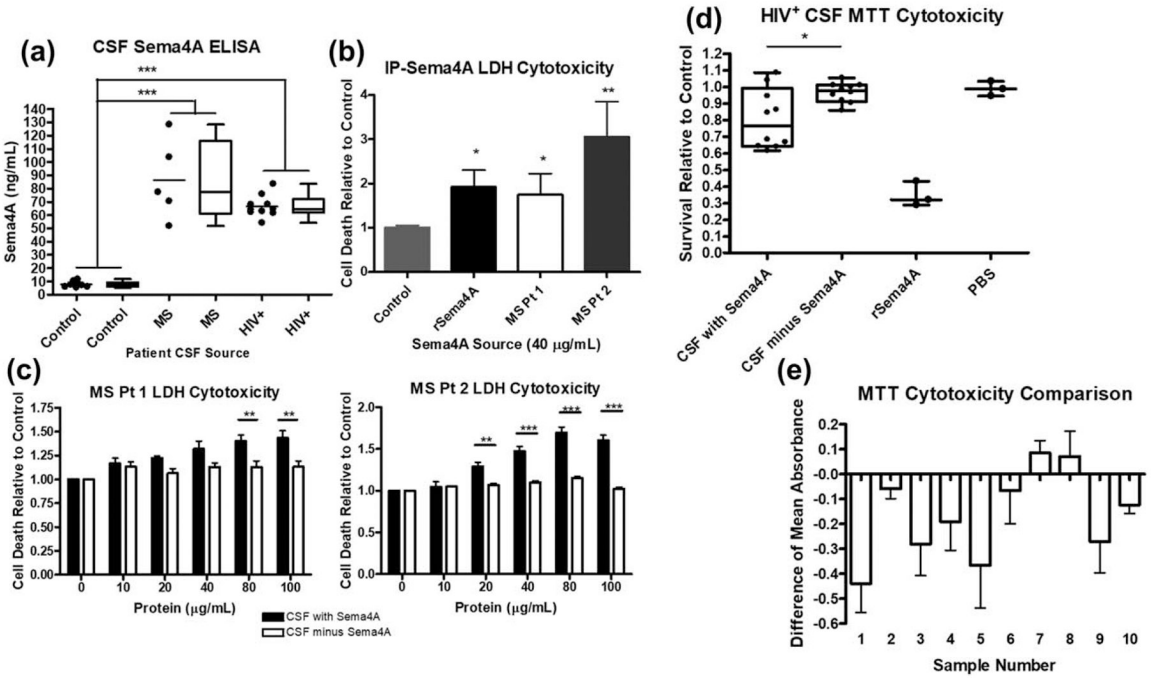

FIGURE 8.

Sema4A from the CSF of patients with multiple sclerosis or HIV+ causes oligodendrocyte cell death. (a) CSF from patients with multiple sclerosis or HIV infection display a higher level of Sema4A. Scatterplot lines represent the mean values while box and whisker plot represents the median and interquartile range. (b) Sema4A isolated from the CSF of MS patients is cytotoxic to mature MO3.13 cells, comparable to the commercially available recombinant Sema4A (rSema4A). Negative control used in this study was PBS. (c) CSF before and after Sema4A immunoprecipitation was applied to mature MO3.13 cells, demonstrating that CSF with Sema4A causes cell death. Two-way ANOVA with Bonferroni's post hoc comparison was used to assess statistical significance. Means are from three biological replicates ± *SD*, *$p < .05$, **$p < .01$, ***$p < .001$. (d) Complete CSF from HIV^+ individuals applied at 100 μg/ml total protein to mature MO3.13 cells causes cytotoxicity, compared with CSF after Sema4A immunoprecipitation, recombinant Sema4A, and PBS control. Mann-Whitney test was used to assess statistical significance between the CSF with Sema4A and CSF minus Sema4A groups; *$p = .0433$. rSema4A and PBS controls are shown for comparison. (e) Individual differences in the mean cytotoxicity between each CSF sample. Differences were calculated as (Mean Absorbance of CSF with Sema4A)-(Mean Absorbance of CSF minus Sema4A)